Supporting information

Hydroxynitrile lyases covalently immobilized in continuous flow microreactors

Michelle P. van der Helm,[a,b,#] Paula Bracco,[a,#] Hanna Busch,[a] Katarzyna Szymańska,*[,b] Andrzej B. Jarzębski,[b,c] and Ulf Hanefeld*[,a]

[a] Biocatalysis, Department of Biotechnology, Delft University of Technology, Van der Maasweg 9, 2629 HZ Delft, The Netherlands

[b] Department of Chemical Engineering and Process Design, Silesian University of Technology, Ks. M. Strzody 7, 44-100 Gliwice, Poland

[c] Institute of Chemical Engineering, Polish Academy of Sciences, Baltycka 5, 44-100 Gliwice, Poland

[#] These authors contributed equally to this work.

***Corresponding Author:** Ulf Hanefeld
Tel: +31(0)15-2789304; Fax: +31(0)15-2781415; Email: U.Hanefeld@tudelft.nl.
Biocatalysis, Department of Biotechnology, Delft University of Technology, Van der Maasweg 9, 2629 HZ Delft, The Netherlands

***Corresponding Author:** Katarzyna Szymańska
Tel: +48322371266; Fax: +48322371461; E-mail: Katarzyna.Szymanska@polsl.pl
Department of Chemical Engineering and Process Design, Silesian University of Technology, Ks. M. Strzody 7, 44-100 Gliwice, Poland

Table of Contents

A. PyMOL characterization

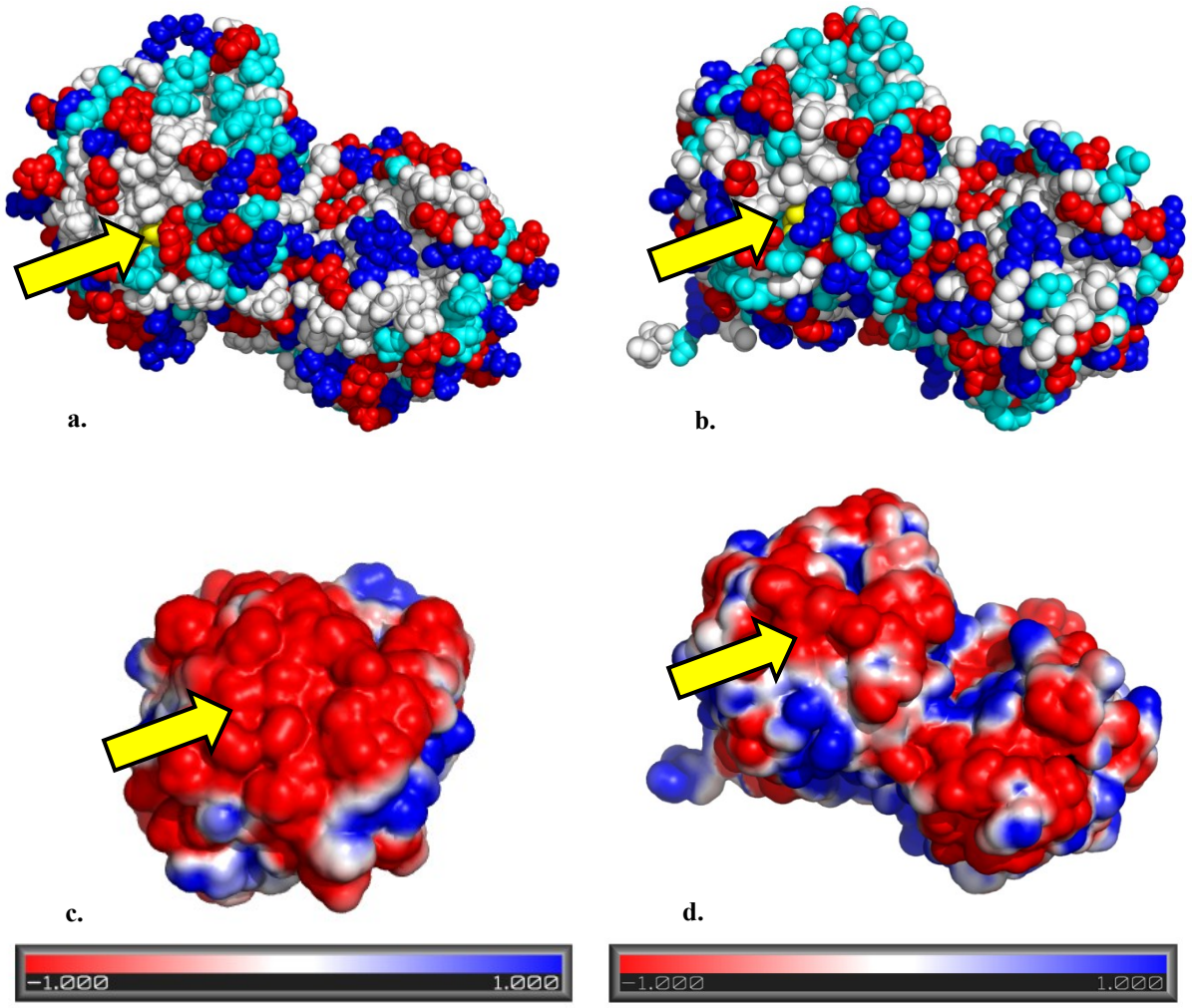

Figure S1: a. *Hb*HNL homodimer amino acid composition. b. *Me*HNL homodimer amino acid composition. Hydrophobic residues are shown in white, polar residues in cyan, basic residues in blue and acid residues in red. The yellow arrow indicates the active site entrance with catalytic triad residues (Ser 80, His 235/236 and Asp 207/208 [1]) shown in yellow, which are partially hidden inside the enzyme structure. c. Poisson–Boltzmann electrostatic surface potential of *Hb*HNL asymmetric unit. d. Poisson–Boltzmann electrostatic surface potential of *Me*HNL homodimer. The solvent accessible surface is shown and water molecules are hidden. Areas in red are negatively charged, areas in blues are positively charged and white areas are neutral at pH 7.0. The yellow arrow represents the active site entrance. The calculation was performed with the PyMOL Molecular Graphics System built-in Adaptive Poisson-Boltzmann Solver (ABPS) plugin [2]. X-ray structures 3C6X [3] and 1DWP [4] were obtained from the PDB [5]. Figures were reconstructed with the PyMOL Molecular Graphics System [6]. N.B. The *Hb*HNL homodimer image was constructed by duplication of the asymmetric unit structural data with the 'symexp' command.

B. TEM MCF carrier

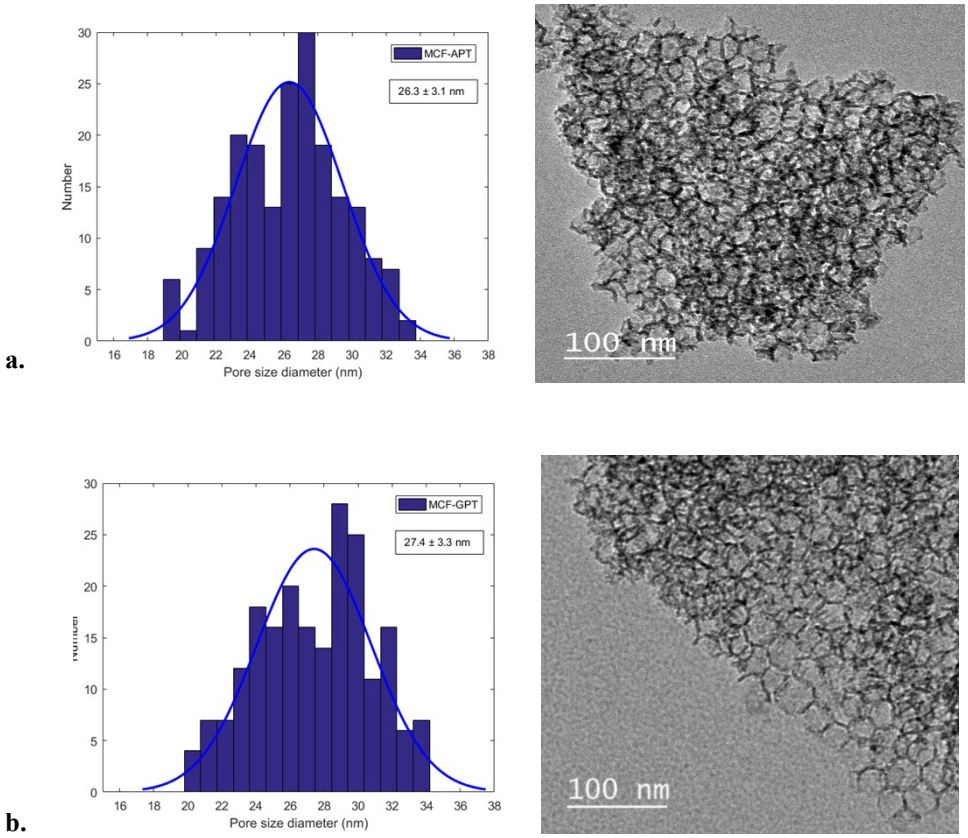

Figure S2: a. MCF-APT. b. MCF-GPT. Histograms with pore size diameter (d_p in nm) distribution fit, created from TEM images with number of data points (n) > 200 (distance measurements and plotting were carried out with ImageJ and MATLAB). Reported error values are standard deviations with n > 200. Representative TEM images are provided on the right.

C. Covalent enzyme immobilization

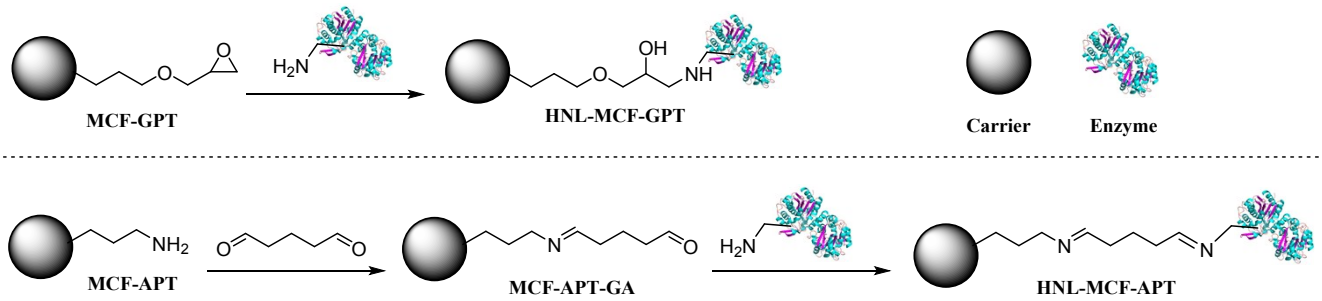

Scheme S1: Schematic covalent enzyme immobilization by reacting the epoxy or amino groups of the MCF carrier with the surface lysine groups of the enzyme (*Hb*HNL or *Me*HNL). Amino groups of MCF-APT are first activated with a glutaraldehyde tether, generating a Schiff's base (MCF-APT-GA).

D. TGA MCF carriers

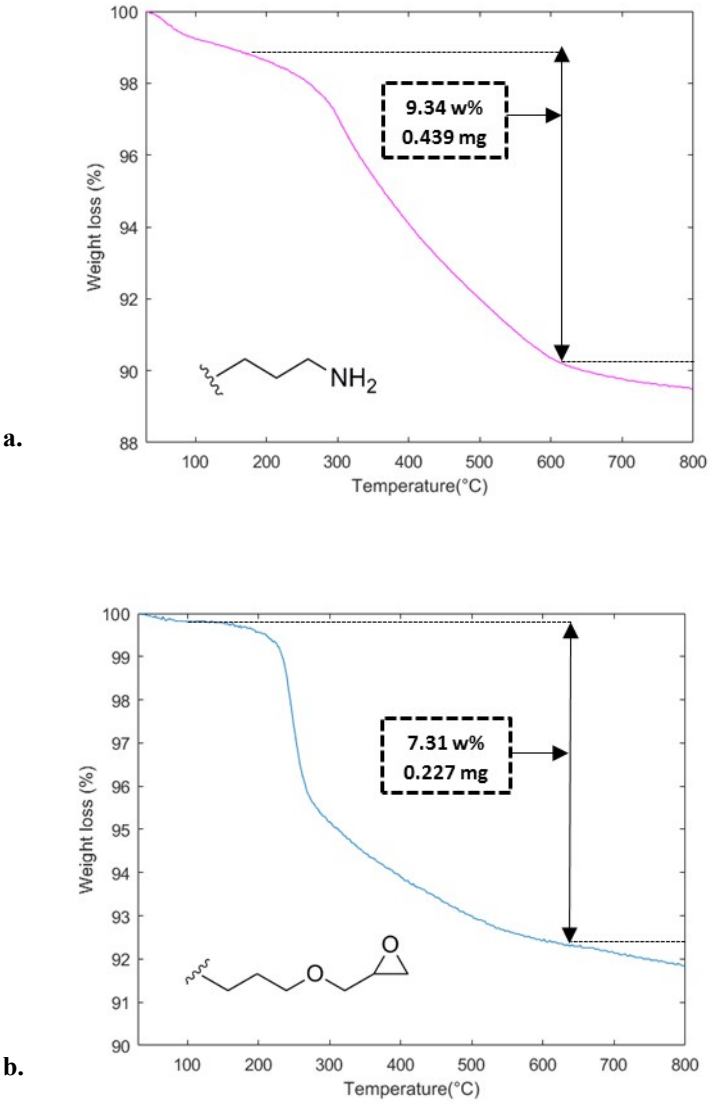

Figure S3: a. TGA curve of MCF-APT. b. TGA curve of MCF-GPT. The black dashed boxes indicate the organic weight loss.

E. FTIR immobilized enzymes

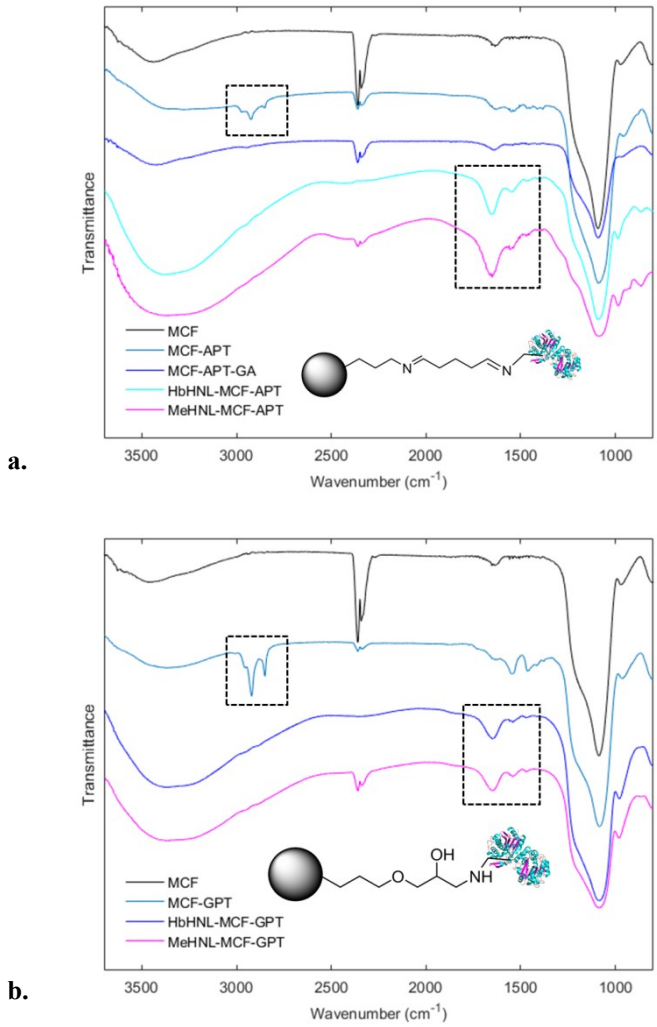

Figure S4: Immobilized enzymes FTIR spectra overlay: a. *Hb*HNL-MCF-APT and *Me*HNL-MCF-APT. MCF-APT-GA is the glutaraldehyde activated carrier, MCF-APT the amino functionalized carrier and MCF the carrier without functional group b. *Hb*HNL-MCF-GPT and *Me*HNL-MCF-GPT. MCF-GPT is the epoxy functionalized carrier and MCF the carrier without functionality. The black dashed box on the left represents the methylene stretching vibrations of the functionalized carriers and the box on the right indicates the vibrations of protein secondary amides. Spectral data were normalized.

F. TGA immobilized enzymes

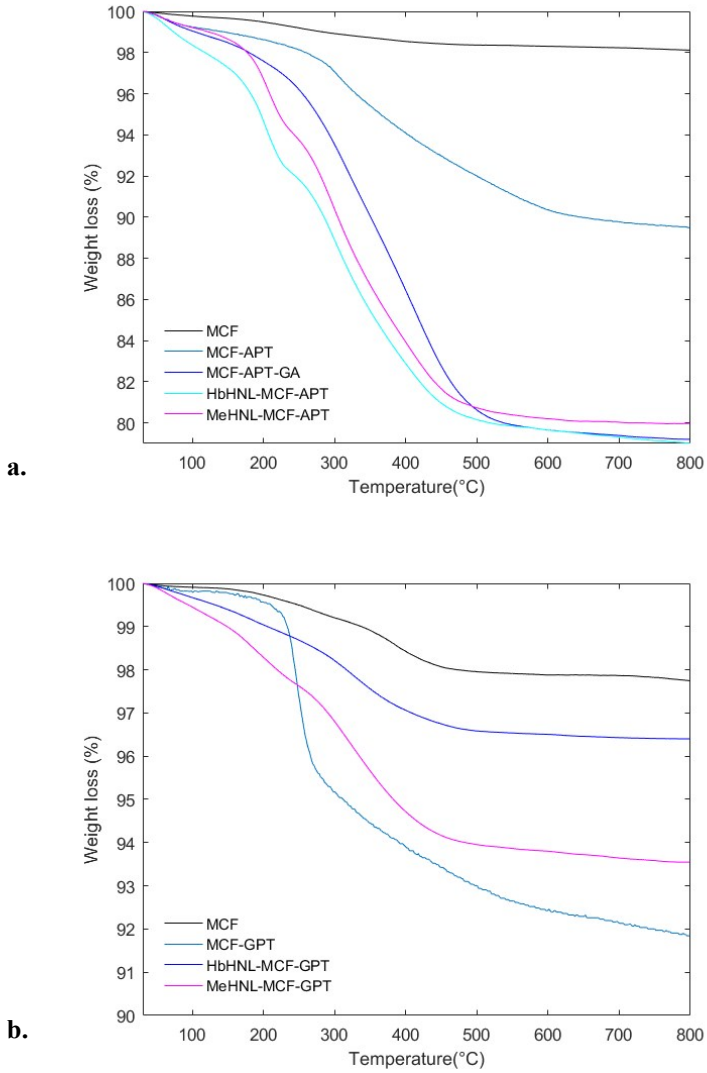

Figure S5: a. TGA overlay curve of *Hb*HNL-MCF-APT and *Me*HNL-MCF-APT. MCF-APT-GA is the glutaraldehyde activated carrier, MCF-APT the amino functionalized carrier and MCF the carrier without functional group b. TGA overlay curve of *Hb*HNL-MCF-GPT and *Me*HNL-MCF-GPT. MCF-GPT is the epoxy functionalized carrier and MCF the carrier without functionality.

G. TEM immobilized enzymes

a.

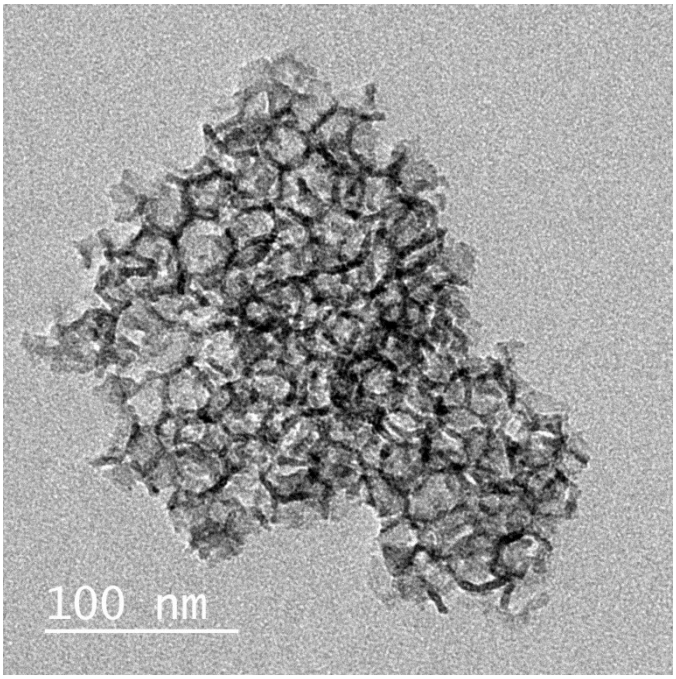

b.

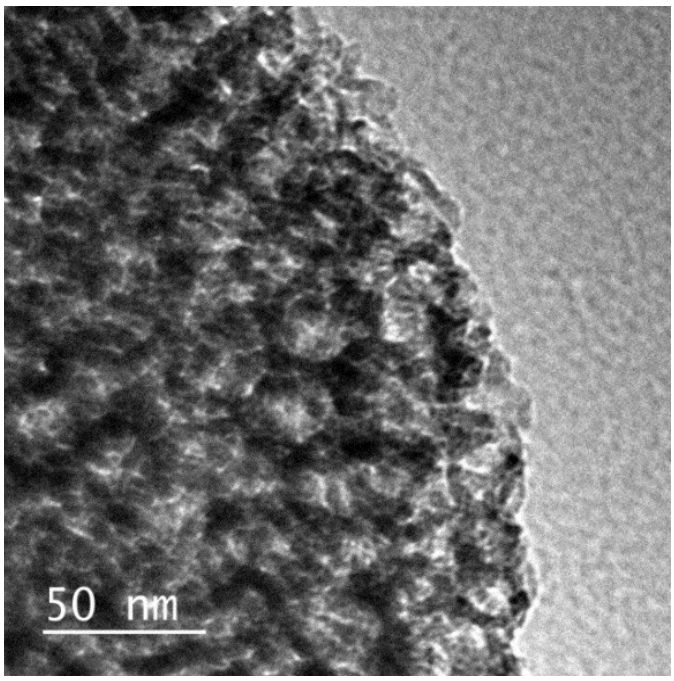

Figure S6: TEM images. a. Functionalized MCF carrier (MCF-APT) before immobilization. b. Functionalized MCF (MCF-APT) carrier after immobilization with *Hb*HNL.

H. SEM immobilized enzymes

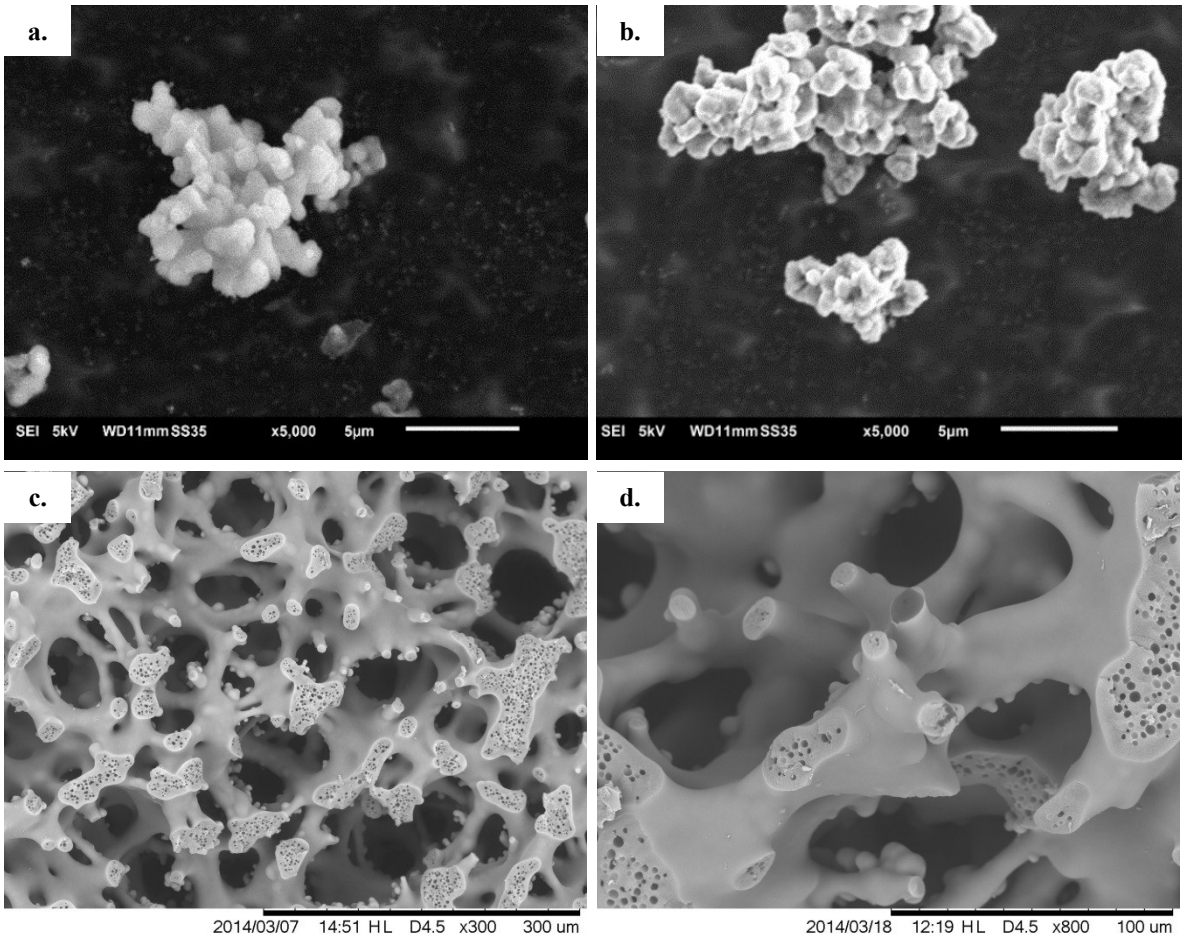

Figure S7: SEM images. a. Functionalized MCF carrier (MCF-APT) before immobilization. b. Functionalized MCF carrier (MCF-APT) after immobilization with *Hb*HNL. c. Silica monolith structure before immobilization low magnification. d. Silica monolith structure before immobilization high magnification

I. Batch reaction synthesis of (*S*)-mandelonitrile by *Hb*HNL-MCF-APT

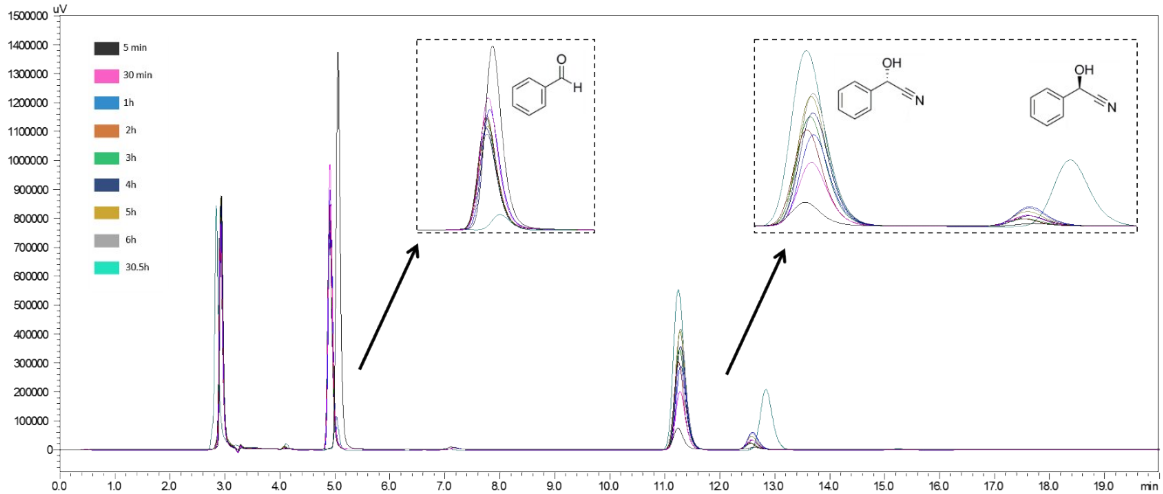

Figure S8: Reaction profile for (*S*)-Mandelonitrile (**(*S*)-2**) synthesis: *Hb*HNL-MCF-APT (50 mg; 2.5 mg total protein; 150 U) rinsed with citrate phosphate buffer (pH 5.0, 50 mM), 2 mL HCN in MTBE (1.5-2 M) saturated with citrate phosphate buffer (pH 5.0, 50 mM), substrate benzaldehyde (**1**) 100 µL (1 mmol), ISTD 1 (1,3,5-triisopropylbenzene) 27.5 µL (0.1 mmol), shaken at 1000 rpm at room temperature (18-22 °C) under nitrogen atmosphere. Reaction was monitored for 30.5 h with HPLC.

J. Background reaction batch system with carrier

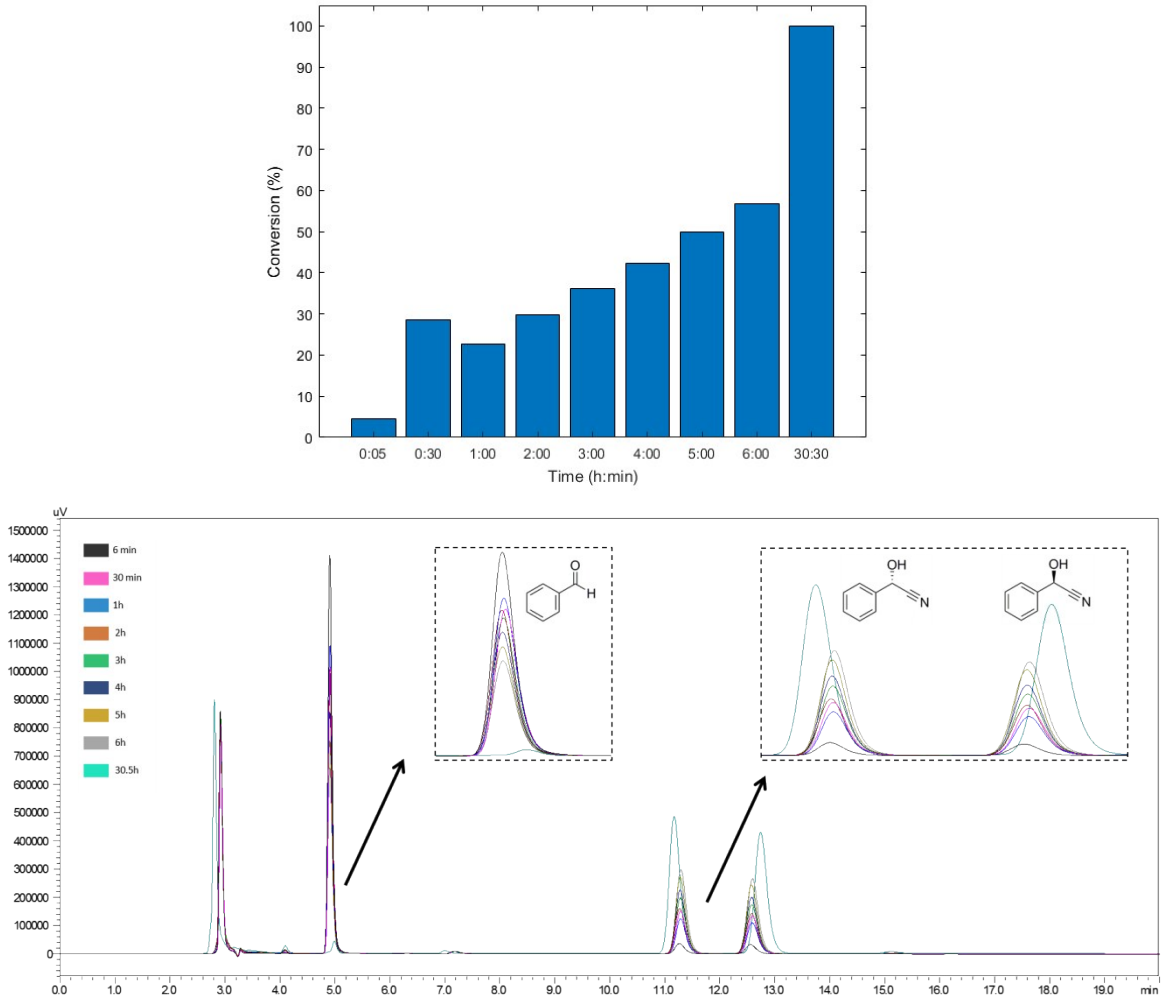

Figure S9: Blank reaction profile (*S*)-Mandelonitrile (**(*S*)-2**) synthesis with carrier: 50 mg glutaraldehyde activated MCF-APT (without enzyme) rinsed with citrate phosphate buffer (pH 5.0, 50 mM), 2 mL HCN in MTBE (1.5-2 M) saturated with citrate phosphate buffer (pH 5.0, 50 mM), benzaldehyde (**1**) ±100 µL (1 mmol) ISTD 1 ±27.5 µL (0.1 mmol), shaken at 1000 rpm at room temperature (18-22 °C) under nitrogen atmosphere, indicating the conversion of benzaldehyde (**1**). Reaction was monitored for 30.5 h with HPLC.

K. Background reaction batch system without carrier

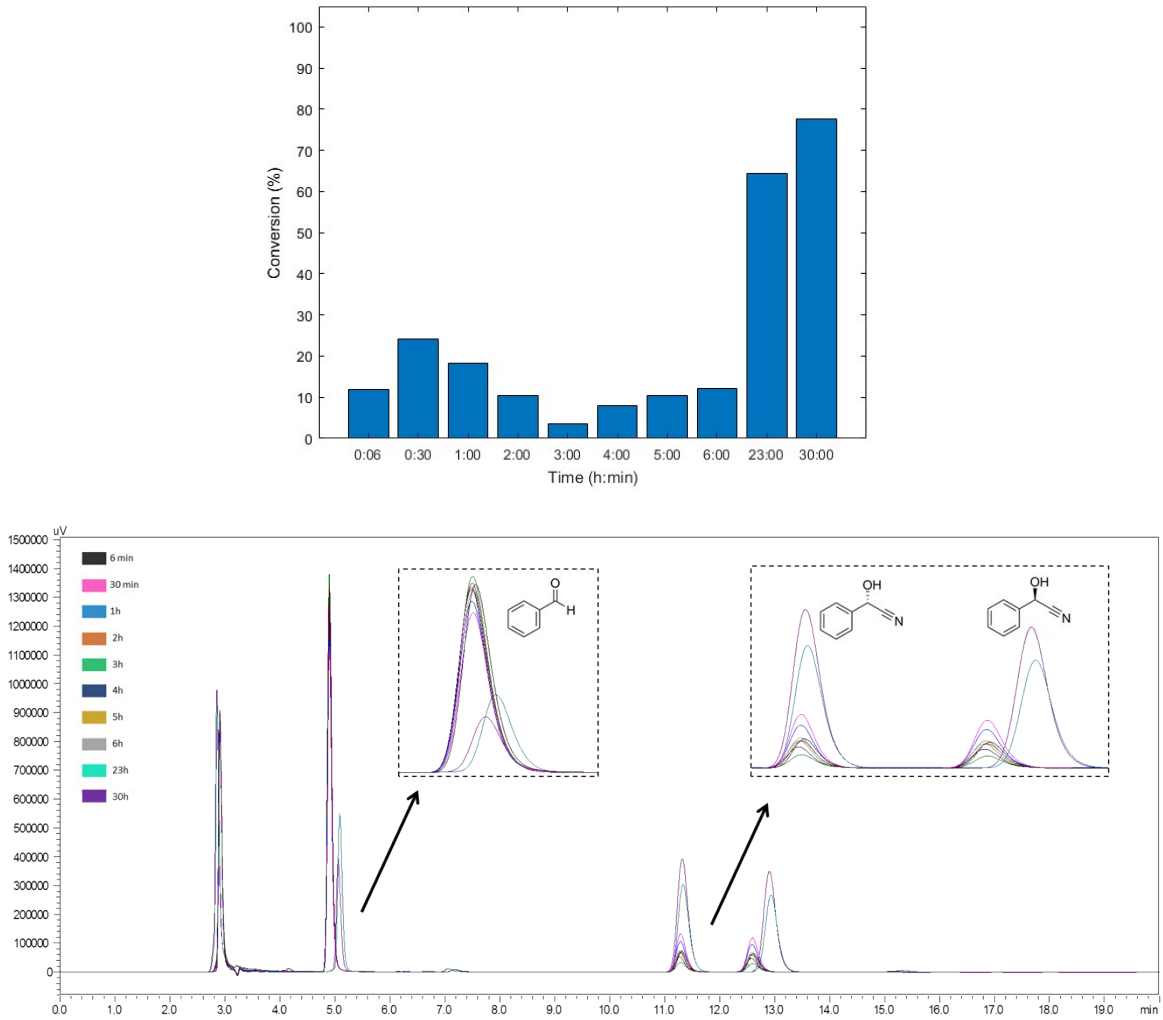

Figure S10: Blank reaction profile (*S*)-Mandelonitrile (**(*S*)-2**) synthesis: 2 mL HCN in MTBE (1.5-2 M) saturated with citrate phosphate buffer (pH 5.0, 50 mM), benzaldehyde (**1**) 100 µL (1 mmol), ISTD 27.5 µL (0.1 mmol), shaken at 1000 rpm at room temperature (18-22 °C) under nitrogen atmosphere, indicating the conversion of benzaldehyde (**1**). Reaction was monitored for 30 h with HPLC.

L. Continuous flow synthesis of (*S*)-mandelonitrile by *Hb*HNL and *Me*HNL

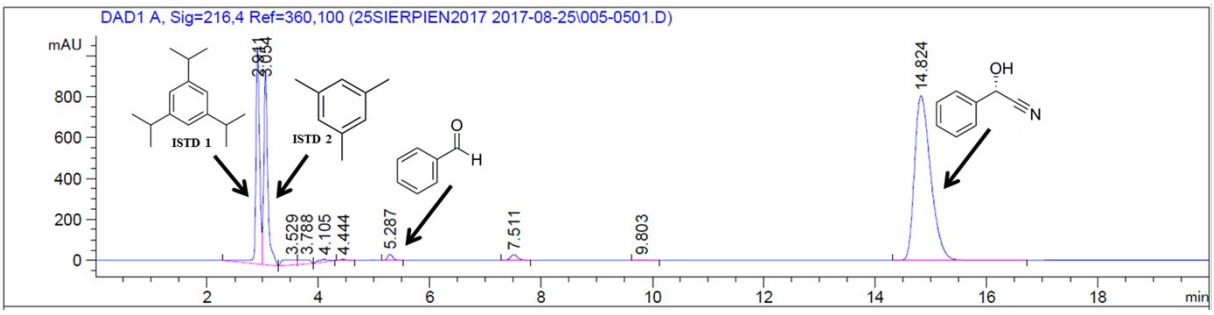

Figure S11: HPLC Chromatogram for the synthesis of (*S*)-mandelonitrile (**(*S*)-2**) with *Hb*HNL-silica monolith (11.3 mg total protein; 1120 U) continuous flow system at 0.075 mL/min flow rate (residence time of 12.8 min). Pump 1 pumps benzaldehyde (**1**) in MTBE (0.50 M, containing 0.066 mM ISTD 1) and pump 2 pumps HCN in MTBE (1.5-2.0 M, containing 0.066 mM ISTD 2 saturated with citrate phosphate buffer (pH 5.0, 50 mM)).

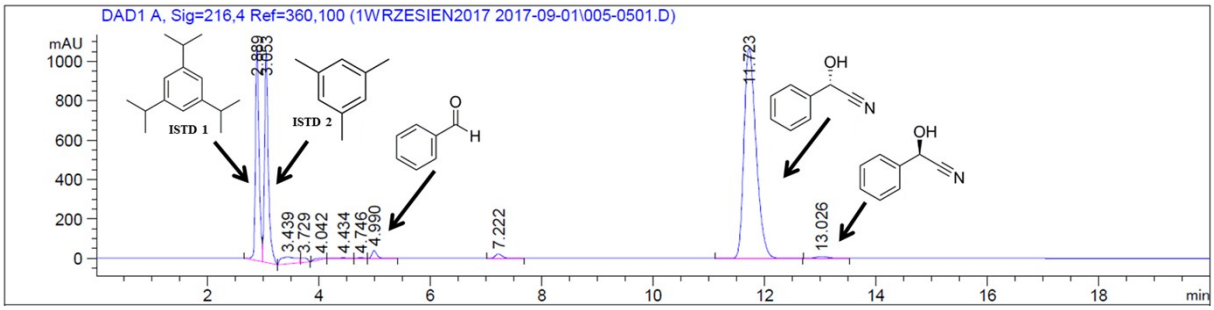

Figure S12: HPLC Chromatogram for the synthesis of (*S*)-mandelonitrile (**(*S*)-2**) with *Me*HNL-silica monolith (17.4 mg total protein; 1310 U) continuous flow system at 0.3 mL/min flow rate (residence time of 3.2 min). Pump 1 pumps benzaldehyde (**1**) in MTBE (0.50 M, containing 0.066 mM ISTD 1) and pump 2 pumps HCN in MTBE (1.5-2.0 M, containing 0.066 mM ISTD 2 saturated with citrate phosphate buffer (pH 5.0, 50 mM)).

M. Background reaction continuous flow system with carrier

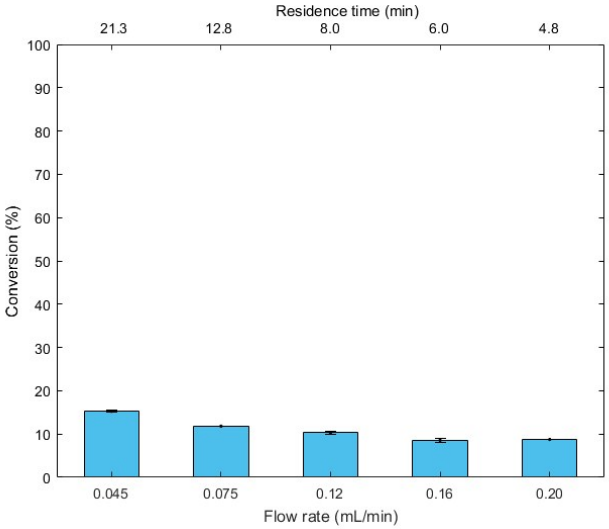

Figure S13: Background reaction of mandelonitrile (***(rac)*-2**) synthesis in continuous flow system (monolith activated with glutaraldehyde - without enzyme). Flow rate is total of two pumps. Pump 1 pumps benzaldehyde (**1**) in MTBE (0.50 M, containing 0.066 mM ISTD 1 and pump 2 pumps HCN in MTBE (1.5-2.0 M, containing 0.066 mM ISTD 2 saturated with citrate phosphate buffer (pH 5.0, 50 mM). Error bars indicate the standard deviation based on triplicate (n=3) HPLC samples (see Experimental section).

N. Explanation for calculation of flow vs batch reaction rates

The specific reaction rate for the continuous flow microreactor system is calculated according to Eq. 1[7, 8]:

$$r_{flow} = \frac{[P] * f}{m_e} \left[\frac{mmol}{min * g}\right] \qquad (1)$$

, in which *[P]* is the product concentration in the reactor outflow (typically in mmol/ml), *f* the flow rate (commonly in ml/min) and m_e the amount of enzyme (in g). Similarly, for the batch reaction the formula for the specific reaction rate is given by Eq. 2[7]:

$$r_{batch} = \frac{n_p}{t * m_e} \left[\frac{mmol}{min * g}\right] \qquad (2)$$

, in which n_p is the amount of product (in mmol) at the specific reaction time, *t* the reaction time (in min) and m_e the amount of enzyme (in g).

Important to mention here is that a comparison of batch and flow reaction rates in this way can only be performed at a similar conversion of substrate, since the product formation rate is a nonlinear function of the conversion and depends on substrate/ product concentrations[7, 8].

O. Gene and protein sequences

HbHNL gene (U40402.1)

ATGGCATTCGCTCATTTTGTTCTTATTCATACCATATGCCACGGTGCATGGATTTG
GCACAAGCTCAAACCCCTCCTTGAGGCACTTGGCCACAAGGTTACTGCACTGGAC
CTTGCAGCAAGCGGCGTTGACCCAAGGCAAATTGAGGAGATTGGCTCATTTGATG
AGTATTCTGAACCCTTGTTGACGTTCTTGGAGGCACTCCCTCCAGGGGAAAAGGT
GATTCTGGTTGGCGAGAGCTGTGGAGGACTCAATATAGCAATTGCTGCTGATAAA
TACTGTGAAAAGATTGCAGCTGCTGTTTTCCACAATTCAGTATTGCCAGACACCG
AGCACTGCCCATCTTACGTCGTGGATAAGCTCATGGAGGTGTTTCCCGACTGGAA
AGACACCACGTATTTTACGTACACTAAAGATGGCAAGGAGATAACTGGATTGAA
ACTGGGCTTCACGCTTCTGAGGGAAAATTTATATACCCTTTGCGGTCCTGAGGAA
TATGAACTGGCGAAGATGTTGACAAGGAAGGGATCATTATTTCAAAATATTTTAG
CTAAGCGACCATTCTTCACTAAGGAAGGTTACGGATCGATTAAGAAAATTTATGT
GTGGACCGACCAAGACGAAATATTTTTACCTGAATTTCAACTCTGGCAAATAGAA
AACTATAAACCAGACAAGGTTTATAAGGTCGAAGGTGGAGATCATAAATTGCAG
CTTACAAAGACTAAGGAGATCGCTGAAATTCTCCAAGAGGTGGCTGATACCTATA
AT

HbHNL protein (XP_021647581.1)

MAFAHFVLIHTICHGAWIWHKLKPLLEALGHKVTALDLAASGVDPRQIEEIGSFDEYS
EPLLTFLEALPPGEKVILVGESCGGLNIAIAADKYCEKIAAAVFHNSVLPDTEHCPSYV
VDKLMEVFPDWKDTTYFTYTKDGKEITGLKLGFTLLRENLYTLCGPEEYELAKMLTR
KGSLFQNILAKRPFFTKEGYGSIKKIYVWTDQDEIFLPEFQLWQIENYKPDKVYKVEG
GDHKLQLTKTKEIAEILQEVADTYN

MeHNL gene

ATGGTGACCGCACATTTTGTTCTGATTCATACCATTTGTCATGGTGCATGGATTTG
GCATAAACTGAAACCGGCACTGGAACGTGCCGGTCATAAAGTTACCGCACTGGA
TATGGCAGCAAGCGGTATTGATCCGCGTCAGATTGAACAAATTAATAGCTTTGAT
GAATATAGCGAACCGCTGCTGACCTTTCTGGAAAAACTGCCGCAGGGTGAAAAA
GTTATTATTGTGGGTGAAAGCTGTGCCGGTCTGAATATTGCAATTGCAGCCGATC
GTTATGTTGATAAAATTGCCGCAGGCGTGTTTCATAATAGCCTGCTGCCGGATAC
CGTTCATAGCCCGAGCTATACCGTTGAAAAACTGCTGGAAAGCTTTCCGGATTGG
CGTGATACCGAATATTTCACCTTTACCAATATTACAGGCGAAACCATTACCACCA
TGAAACTGGGTTTTGTTCTGCTGCGTGAAAACCTGTTTACCAAATGCACCGATGG
TGAATATGAACTGGCGAAAATGGTTATGCGTAAAGGTAGCCTGTTTCAGAATGTT
CTGGCACAGCGTCCGAAATTTACCGAAAAAGGCTATGGCAGCATTAAAAAAGTG
TATATTTGGACCGATCAGGATAAAATTTTTCTGCCGGATTTTCAGCGTTGGCAGAT
TGCAAATTATAAACCGGATAAAGTGTATCAGGTTCAGGGTGGTGATCATAAACTG
CAGCTGACGAAAACCGAAGAAGTTGCACATATTCTGCAGGAAGTTGCAGACGCA
TACGCA

MeHNL protein (XP_021633598.1)

MVTAHFVLIHTICHGAWIWHKLKPALERAGHKVTALDMAASGIDPRQIEQINSFDEY
SEPLLTFLEKLPQGEKVIIVGESCAGLNIAIAADRYVDKIAAGVFHNSLLPDTVHSPSY
TVEKLLESFPDWRDTEYFTFTNITGETITTMKLGFVLLRENLFTKCTDGEYELAKMV
MRKGSLFQNVLAQRPKFTEKGYGSIKKVYIWTDQDKIFLPDFQRWQIANYKPDKVY
QVQGGDHKLQLTKTEEVAHILQEVADAYA

P. SDS-PAGE analysis

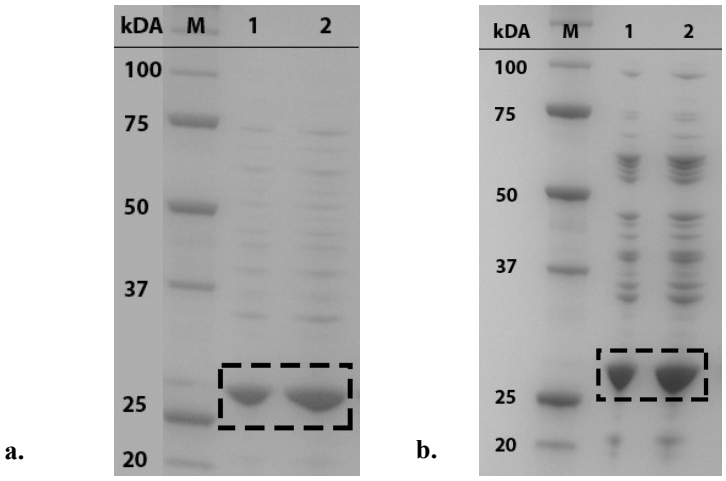

Figure S14: SDS-PAGE (12% Bis-Tris, MOPS Buffer): a. *Hb*HNL after enzyme isolation with purity of 88%. The black dashed box represents the protein bands of *Hb*HNL (30 kDa [9]). b. *Me*HNL after enzyme isolation with purity of 55%. The black dashed box represents the protein bands of *Me*HNL (28-30 kDa [9]). M = Marker, 1 = 5 µl loading and 2 = 10 µl loading. The purity estimation of the total protein concentration was performed with a quantitative evaluation of the SDS-PAGE with GeneTools software, making use of the Precision Plus Protein™ Unstained Standards weight calibration (Bio-Rad).

Q. Reaction set-ups

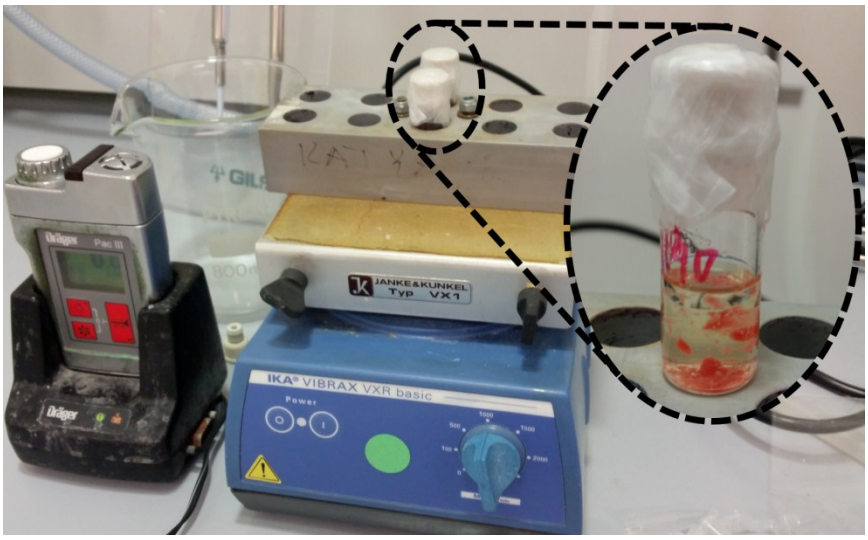

Figure S15: Batch reaction set-up for (*S*)-mandelonitrile (**(*S*)-2**) synthesis with *Hb*HNL-MCF-APT using 4 mL reaction vials sealed with a septum.

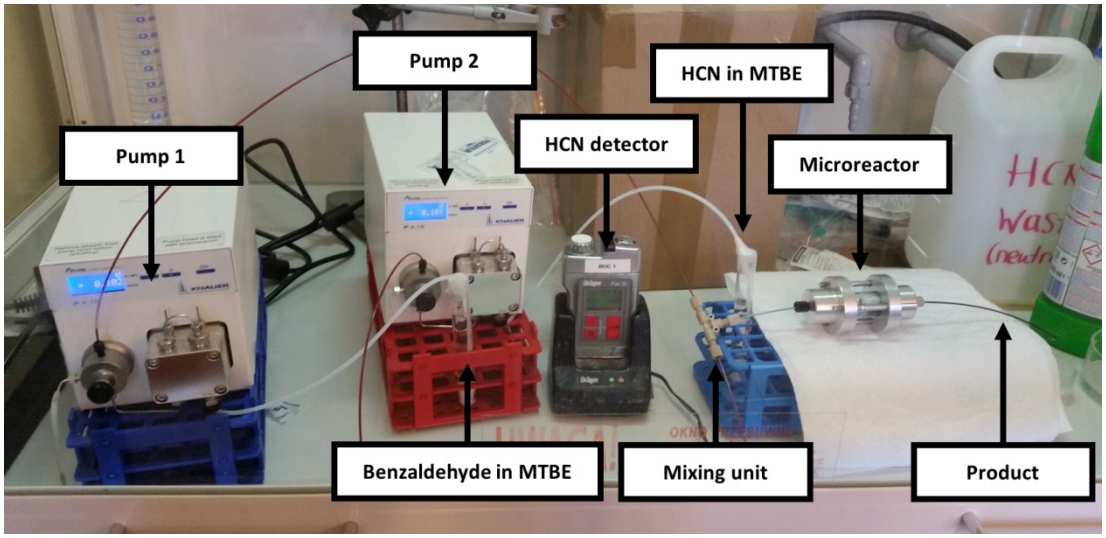

Figure S16: Continuous flow reaction set-up (in buffer saturated organic solvent) for (*S*)-mandelonitrile (**(*S*)-2**) synthesis using two high pressure pumps and a mixing unit.

R. NMR spectra

^{1}H NMR and ^{13}C NMR data for (*rac*)-mandelonitrile (**(*rac*)-2**) are in accordance with literature [10]. ^{1}H NMR (400 MHz, $CDCl_3$) δ: 7.47-7.39 (m, 5H), 5.46 (s, 1H), 3.66 (s, 1H). ^{13}C NMR (100.5 MHz, $CDCl_3$) δ: 63.5, 118.9, 126.7, 129.2, 129.8, 135.1.

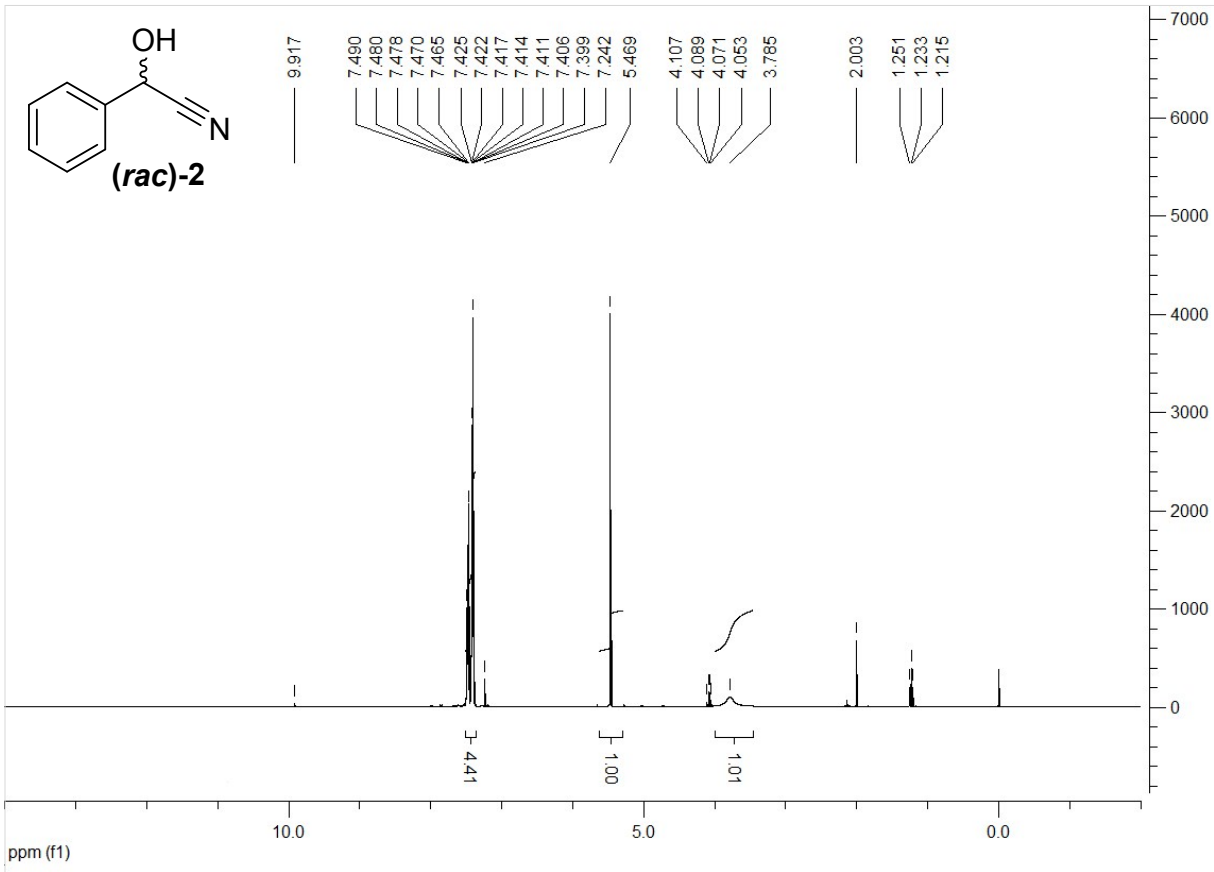

Figure S17: ^{1}H NMR spectrum of (*rac*)-mandelonitrile (**(*rac*)-2**).

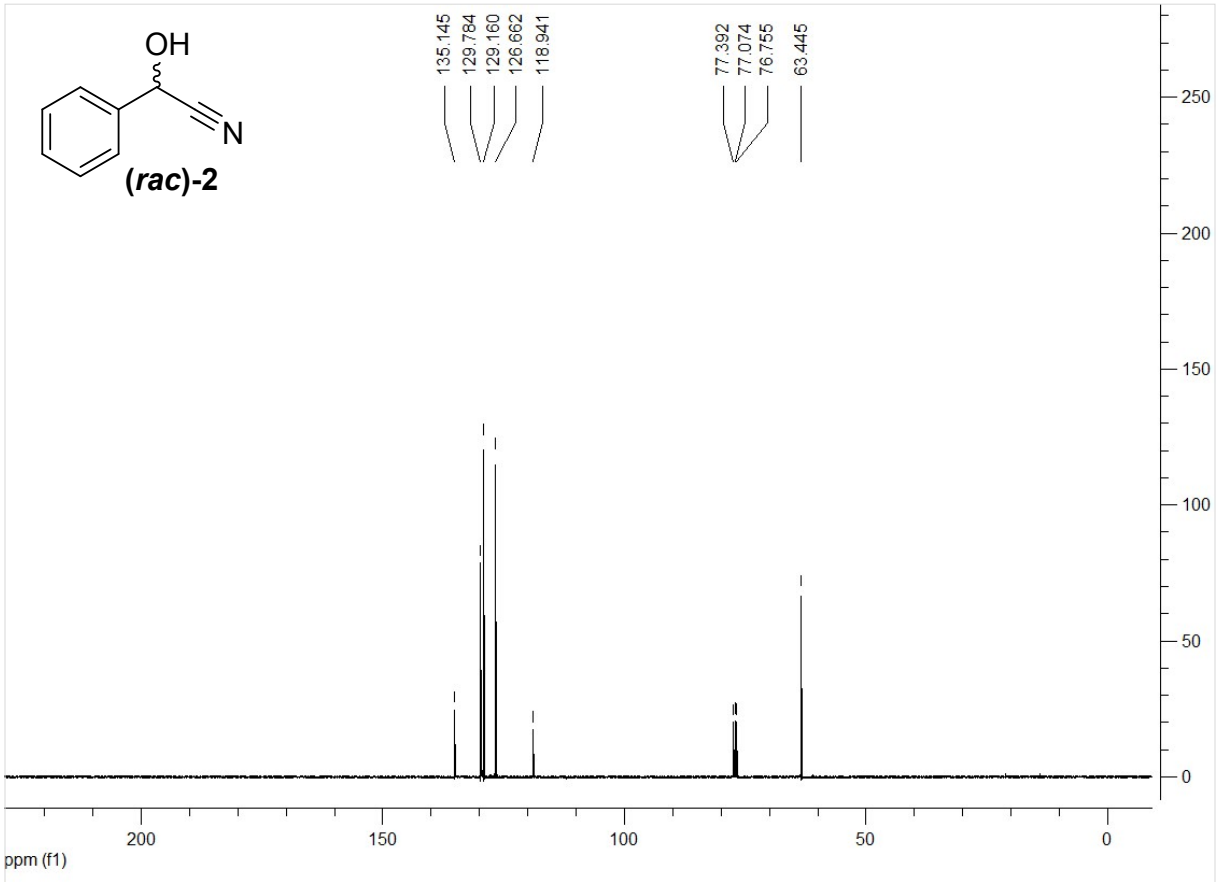

Figure S18: ^{13}C NMR spectrum of (*rac*)-mandelonitrile (**(*rac*)-2**).

S. References

1. K. Gruber, G. Gartler, B. Krammer, H. Schwab and C. Kratky, *J. Biol. Chem.*, 2004, **279**, 20501-20510.
2. N. A. Baker, D. Sept, S. Joseph, M. J. Holst and J. A. McCammon, *Proc. Natl. Acad. Sci.*, 2001, **98**, 10037-10041.
3. A. Schmidt, K. Gruber, C. Kratky and V. S. Lamzin, *J. Biol. Chem.*, 2008, **283**, 21827-21836.
4. H. Lauble, S. Förster, B. Miehlich, H. Wajant and F. Effenberger, *Acta Crystallogr., Sect D: Biol. Crystallogr.*, 2001, **57**, 194-200.
5. H. M. Berman, J. Westbrook, Z. Feng, G. Gilliland, T. N. Bhat, H. Weissig, I. N. Shindyalov and P. E. Bourne, *Nucleic Acids Res.*, 2000, **28**, 235-242.
6. Schrödinger, LLC, *Journal*, 2015.
7. C. Csajagi, G. Szatzker, E. R. Tőke, L. Uerge, F. Darvas and L. Poppe, *Tetrahedron: Asymmetry*, 2008, **19**, 237-246.
8. L. Tamborini, P. Fernandes, F. Paradisi and F. Molinari, *Trends Biotechnol.*, 2017, DOI: https://doi.org/10.1016/j.tibtech.2017.09.005.
9. F. Effenberger, S. Förster and H. Wajant, *Curr. Opin. Chem. Biol.*, 2000, **11**, 532-539.
10. W.-B. Yang and J.-M. Fang, *J. Org. Chem.*, 1998, **63**, 1356-1359.